Since January 2020 Elsevier has created a COVID-19 resource centre with free information in English and Mandarin on the novel coronavirus COVID-19. The COVID-19 resource centre is hosted on Elsevier Connect, the company's public news and information website.

Talanta 253 (2023) 123981

Contents lists available at ScienceDirect

Talanta

journal homepage: www.elsevier.com/locate/talanta

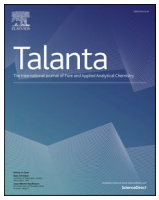

Evaluation of the interaction between SARS-CoV-2 spike glycoproteins and the molecularly imprinted polypyrrole

Vilma Ratautaite [a,c], Raimonda Boguzaite [a], Ernestas Brazys [b], Deivis Plausinaitis [b], Simonas Ramanavicius [b,c], Urte Samukaite-Bubniene [a,b], Mikhael Bechelany [d], Arunas Ramanavicius [a,b,*]

[a] Department of Nanotechnology, Center for Physical Sciences and Technology, Sauletekio av. 3, Vilnius, LT-10257, Lithuania
[b] Department of Physical Chemistry, Institute of Chemistry, Faculty of Chemistry and Geosciences, Vilnius University, Naugarduko str. 24, Vilnius, LT-03225, Lithuania
[c] Department of Electrochemical Material Science, Center for Physical Sciences and Technology, Sauletekio av. 3, Vilnius, LT-10257, Lithuania
[d] Institut Européen des Membranes, IEM, UMR 5635, University of Montpellier, CNRS, ENSCM, 34090, Montpellier, France

ARTICLE INFO

Keywords:
Molecularly imprinted polymers (MIPs)
Polypyrrole (Ppy)
Integrated cottrell equation
Anson plot
SARS-CoV-2 spike glycoprotein

ABSTRACT

The SARS-CoV-2 spike glycoprotein (SARS-CoV-2-S) was used as a template molecule and polypyrrole (Ppy) was applied as an electro-generated conducting polymer, which was acting as a matrix for the formation of molecular imprints. Two types of Ppy-layers: molecularly imprinted polypyrrole (MIP-Ppy) and non-imprinted polypyrrole (NIP-Ppy) were electrochemically deposited on the working platinum electrode. The performance of electrodes modified by MIP-Ppy and NIP-Ppy layers was evaluated by pulsed amperometric detection (PAD). During the assessment of measurement results registered by PAD, the integrated Cottrell equation (Anson plot) was used to calculate the amount of charge passed through the MIP-Ppy and NIP-Ppy layers. The interaction between SARS-CoV-2 spike glycoproteins and molecularly imprinted polypyrrole (MIP-Ppy) was assessed by the Anson plot based calculations. This assessment reveals that SARS-CoV-2-S glycoproteins are interacting with MIP-Ppy more strongly than with NIP-Ppy.

1. Introduction

Molecularly imprinted polymers (MIPs) are artificially formed polymer structures suitable for the design of highly specific, selective, and sensitive analytical systems. Conducting polymers are frequently used for the development of MIPs and can be formed by electrochemical methods. Rather simple procedure of the electrochemical MIP manufacturing process and the ability to modify, and ameliorate characteristics of the MIP with dopants or by electrochemical parameters have attracted significant attention of researchers. However, the comprehensibility of the interaction peculiarities between the molecule of interest and imprinted cavity formed within the MIP is still relevant. Molecularly imprinted polymers (MIPs) are used in the recognition process because the way by which they operate can be described as synthetic analogs to the natural, biological antibody-antigen, or receptor-ligand-based systems. The process of MIP fabrication usually involves steps such as the polymerization of monomers in the presence of a template molecule, extraction of the template molecules after polymerization, and afterward, MIP-based structures are ready for application in electrochemical MIP-based sensors [1–3]. During the polymerization, the template molecule forms an imprint within the polymer, which creates a cavity complementary to template molecule. Therefore, such cavities enables the selective recognition/binding of template molecules.

MIPs can be successfully designed for the recognition of various types of small molecular weight template molecules [1,4–7] imprinted within different polymers, including polypyrrole (Ppy) [4,5,8], polyaniline [8–10], and many others. These MIPs can be used in analytical systems based on different analytical techniques [4,11–13]. Some challenges and limitations of these MIPs are well discussed in several recently published review articles [2,3,14–18]. But among the different template molecules, the imprinting of macromolecules has some specific features [14,19,20]. Kan et al. [20] identified three limitations that are the most critical during protein imprinting. In particular, it is difficult to

* Corresponding author. Department of Nanotechnology, Center for Physical Sciences and Technology, (Vilnius University), Sauletekio av. 3, Vilnius, LT-10257, Lithuania.
E-mail address: arunas.ramanavicius@chf.vu.lt (A. Ramanavicius).

https://doi.org/10.1016/j.talanta.2022.123981
Received 30 June 2022; Received in revised form 24 September 2022; Accepted 28 September 2022
Available online 6 October 2022

remove the template protein from the bulk polymer matrix after the polymerization. Furthermore, organic solvents are often used in the formation of MIPs, although, they are unsuitable for the synthesis of protein-imprinted MIPs due to the poor solubility of the protein molecule in these solvents and possible denaturation of proteins in organic solvents. Due to this shortage, electrochemical polymerization is a better choice, because it can be performed in aqueous solutions. In this case, the environment is less polluted, therefore, it perfectly meets the principles of the green chemistry [21]. Finally, the size and structural complexity of the protein results in a more significant non-specific binding [20].

Some conducting polymers have been molecularly imprinted with various high molecular mass biomolecules including proteins [22–33], DNA [34,35], or even bacteria [36–38]. Polypyrrole has previously been molecularly imprinted by glycoproteins of virus [33], bovine hemoglobin [20,39,40], bovine serum albumin [41], prostate-specific antigen [42], cardiac troponin-I [43], and cardiac troponin T [44]. It is noteworthy to mention that cyclic voltammetry (CV) [20,41–44], differential pulse voltammetry (DPV) [20,39–41,43,44], and electrochemical impedance spectroscopy (EIS) [20,39–41,43] in presence of redox probe $[Fe(CN)_6]^{3-}/[Fe(CN)_6]^{4-}$ were the most frequently used electrochemical methods for the evaluation of the MIPs imprinted with proteins. The MIPs based on polypyrrole with bovine leukemia virus glycoproteins imprints [33] and SARS-CoV-2 spike glycoproteins [45] were evaluated by pulsed amperometric detection (PAD) method in the absence of ferrocyanide-ferricyanide system as a redox probe. According the review of Faria et al. [46], such an analytical system should be classified as a type of non-faradaic sensor. In such case, charging and discharging of the double-layer capacitance are playing the most important role. At the same time, it is important to keep in mind that by changing the potential, the charging and the discharging of the conducting polymers occur. This effect was well discussed by Heinze et al. [47]. The electrochemical charging process of conducting polymers should be described by a sequence of discrete but overlapping redox steps. By changing the potential, there are more effects observed and the volume change is one of them. These effects are induced by the oxidation and the reduction of the polymer [48–50].

SARS-CoV-2 protein plays a key role in the cell receptor recognition/binding and penetration of the SARS-CoV-2 virus through the cell membrane. Aspects of electrochemical determination methods of proteins employing MIPs are especially interesting due to the recent widespread of the SARS-CoV-2 virus causing the COVID-19 disease. Recently some studies employing MIP-technology for SARS-CoV-2 spike glycoprotein were published [45,51–56]. The sensors mentioned in the literature differ in their primary system, composition, and preparation method, however, all of them are characterized by low cost, fast response, and real applicability [52,57,58]. The nucleocapsid, envelope, spike, and membrane proteins of the SARS-CoV-2 virus could be used as template macromolecules during the development of MIPs. Among the here-mentioned proteins, the spike protein SARS-CoV-2-S plays a key role in the cell receptor recognition/binding and the penetration of the SARS-CoV-2 virus through the cell membrane.

In this work, the polypyrrole-based MIP (MIP-Ppy) was developed and applied for the determination of the SARS-CoV-2-S spike glycoprotein to examine in detail complex and little-studied advantages/peculiarities of pulsed amperometric detection as the non-faradaic method. The novelty of the article was based on the application of total charge for the evaluation of the interaction between electrode and analyte. This total charge was calculated according to the integrated Cottrell equation and was plotted, as it was first demonstrated in articles of the F. C. Anson's research group for studies of reactants adsorption on the electrode [59–61]. In honor of this scientist nowadays, the plot of the total charge vs. square of time is called the Anson plot. So, the key idea of this work was based on the application of the Anson plots for elucidation of the interaction between SARS-CoV-2 spike glycoproteins and the molecularly imprinted polypyrrole.

2. Materials and methods

2.1. Chemicals and instrumentation

All chemicals were used as received without further purification. The chemicals were purchased as follows: pyrrole 98% – from *Alfa Aesar* (Germany), sulfuric acid (H_2SO_4; 96%) from *Lachner* (Czech Republic), nitric acid (HNO_3, 63%), sodium hydroxide (NaOH, 98%), and chloroplatinic acid (H_2PtCl_6, 40% Pt) from *Merck* (Germany), potassium phosphate (KH_2PO_4, 98%) from *Honeywell Riedel-de Haen* (Germany), sodium chloride (NaCl, 99,5%), potassium chloride (KCl, 99,5%), and disodium hydrogen phosphate (Na_2HPO_4, 99%) from *Carl Roth* (Germany). SARS-CoV-2 spike glycoproteins were purchased from UAB *Baltymas* (Lithuania).

The experiment was performed using potentiostat/galvanostat Metrohm-Autolab model μAutolabIII/FRA2 μ3AUT71079 controlled by NOVA 2.1.3 software (*EcoChemie*, The Netherlands). All measurements were done in a homemade cell. The total volume of the cell was 250 μL. Three-electrode system consisted of a working electrode (WE) – Pt disk with 1 mm diameter sealed in glass, reference electrode (RE) – Ag/AgCl, and counter electrode (CE) – Pt disk of 2 mm diameter.

2.2. Pretreatment of the working electrode

The working electrode was pretreated according to the procedure described in previous studies [33,62]. Solutions were degassed with a stream of nitrogen (N_2) before use. According to this procedure: 1) the Pt electrode was rinsed with concentrated HNO_3 solution in an ultrasonic bath for 10 min, 2) then rinsed with water, and 3) polished with alumina paste. Later on, 4) it was rinsed with water again and then 5) with 10 M of NaOH, thereafter – 6) with 5 M of H_2SO_4 in an ultrasonic bath for 5 min. 7) Electrochemical cleaning of the electrode was carried out in 0.5 M H_2SO_4 by cycling the potential 20 times in the range between −100 mV and +1200 mV vs. Ag/AgCl at a sweep rate of 100 mV s^{-1}. The bare electrode surface was indicated by a stable cyclic voltammogram. A layer of 'platinum black' was deposited over the working electrode to improve the adhesion of the Ppy layer to the electrode surface [62]. 'Platinum black' was deposited from a 5 mM solution of H_2PtCl_6, 0.1 M of KCl by 10 potential cycles in the range between +500 mV and −400 mV vs. Ag/AgCl at a sweep rate of 10 mV s^{-1}.

2.3. Electrochemical deposition of MIP and NIP layers. Sensor signal evaluation

The electrochemical deposition of the polypyrrole layer was performed in the same electrochemical cell. Non-imprinted polypyrrole (NIP-Ppy) was electrochemically deposited from the polymerization solution containing 0.5 M of pyrrole in PBS with 0.1 M of KCl, pH 7.4. Deposition of molecularly imprinted polypyrrole (MIP-Ppy) was carried out from the polymerization solution containing 0.5 M of pyrrole and 50 μg/mL of SARS-CoV-2 spike glycoprotein in the same PBS with 0.1 M of KCl, pH 7.4. The polymeric layers were formed by a sequence of 20 potential pulses of +950 mV vs. Ag/AgCl for 1 s, between these pulses 0 V vs. Ag/AgCl potential for 10 s was applied [33,62]. MIP-Ppy or NIP-Ppy modified electrodes were immersed in 0.05 M H_2SO_4 solution for 10 min and so the template molecules were extracted. MIP-Ppy or NIP-Ppy layers were incubated for 2 min in the PBS solution in the absence of SARS-CoV-2 spike glycoprotein or the presence of SARS-CoV-2 spike glycoprotein, in a concentration range from 0 μg/mL to 25 μg/mL. Next, MIP-Ppy and NIP-Ppy modified electrodes and interactions with SARS-CoV-2 spike glycoproteins were analyzed with the PAD method: the sequence of 10 potential pulses of +600 mV vs. Ag/AgCl for 2 s, between these pulses 0 V vs. Ag/AgCl was applied for 2 s (Fig. S1 and S2) [33].

3. Results and discussions

As it was described in the experimental part, the MIP-Ppy and NIP-Ppy modified electrodes were evaluated with the PAD method. The obtained amperograms are presented in Fig. 1.

The concentration of the SARS-CoV-2 spike glycoprotein varied from 0 μg/mL to 25 μg/mL. Fig. 1A and B demonstrate the dependence of the amperometric response of MIP-Ppy and NIP-Ppy modified Pt electrodes which were incubated in the SARS-CoV-2 spike glycoprotein containing PBS solution, pH 7.4. The change in the amperometric response is related to the adsorption of less conductive protein molecules on the MIP-Ppy or the NIP-Ppy layer. When SARS-CoV-2 spike glycoprotein concentration in solution increased, the registered amperometric response of both MIP-Ppy and NIP-Ppy-modified Pt electrodes decreased. Before the incubation of the electrode in the SARS-CoV-2 spike glycoprotein-containing solution, higher currents were registered. This effect is determined by the presence of water molecules and electrolyte ions in the places where molecular imprints were formed. After the incubation in the solution containing SARS-CoV-2 spike glycoprotein, the molecules of SARS-CoV-2 spike glycoprotein have replaced the ions of solvent and the electrolyte and thus the current at the potential of +600 mV was decreased. The amperometric response of the last pulses of +600 mV and 0 V from a 10 potential pulses-based sequence applied to MIP-Ppy and NIP-Ppy modified electrodes was selected for a more detailed evaluation (Fig. 2).

The relation of the cumulative charge passed and time in Ppy-based electrochemical sensors obeys the integrated Cottrell equation (1) [59,63]:

$$Q = 2nFAC\sqrt{\frac{D}{\pi}}\sqrt{t} + Q_{d.l.} + Q_{ads.} = k\sqrt{t} + Q_{d.l.} + Q_{ads.} \quad (1)$$

where: Q – total charge (C); n – number of electrons; F – Faraday constant (96,485 C/mol); A – area of the electrode (cm^2); C – concentration (M); D – diffusion coefficient (cm^2/s); t – time (s); $Q_{d.\,l.}$ – the charge of the electrical double layer; $Q_{ads.}$ – charge induced by adsorbed ions.

The cumulative charge in the Cottrell equation corresponds to the charge passed associated with redox activity leading to Faradaic charges ($Q_{F.}$), charging, and discharging of electrode-electrolyte double-layer capacitive charges ($Q_{d.l.}$), and charge changes associated with the adsorbed species ($Q_{ads.}$) [64]. Hence, the plot of Q vs. $t^{½}$ has a linear correlation with the slope k and the intercept corresponding to $Q_{ads.} + Q_{d.\,l.}$. As it was described previously, the absence of specific adsorption of analytes on the surface of the unmodified mercury electrode was indicated by two straight lines with equal slopes that intersect each other at the $Q = 0$ axis [59]. Several studies are appointed to evaluate the adsorption process on the electrode. As stated in a previous study [61], the expected effect of the adsorbed analyte is inducing the increase of the intercept, although the slope remains unchanged. In the other two former articles [61,65], the adsorption process was evaluated by using mercury and the screen-printed electrodes (printed using a carbon-graphite ink). In these studies, it was demonstrated that the slope is proportional to the concentration and the intercept reflects the increasing adsorption. Confirmation that there is no analyte adsorbing on the electrode is based on the Q vs. $t^{½}$ plots, which were registered during potential pulses of different polarity, with equal (but with opposite signs) slopes and intercepts [60]. It was stated, that this might usually be taken as a good evidence for the absence of reactant (or product) adsorption. Another study was appointed to determine the type of adsorbate (reactant or product) on the electrode and the evidence of reactant or product adsorption was based on changes in slope and intercept [66].

The effect described in this study is more complex compared to those presented in literature [59,61,65]. In these studies, a plain electrode without any modification was used. Therefore, it is possible to describe the simplified reaction of the analyte on the electrode in several steps: diffusion of the analyte from the solution to the electrode, electrochemical oxidation-reduction reaction, and then diffusion of the reaction products from the electrode to the solution. Analysis of the slopes and intercepts in the Anson plot may be used for the identification of the adsorption either of the analytes or the reaction products on the electrode. In this study, the Pt electrode was modified with the conducting polymer Ppy that was further imprinted or non-imprinted with glycoprotein. It is noteworthy that by changing the potential, the Ppy layer itself can take part in charging and discharging during the electrochemical oxidation and reduction reaction [47]. On the other hand, the evaluation of charge carrier transfer mechanisms between glucose oxidase and organic semiconductors givesserious insights into the potential transfer of charge carriers (holes and electrons) [67]. These insights make the analysis of the amperograms complex but still possible to describe in the terms suggested by Anson.

The Anson plots are depicted (Fig. 3A and D, and Fig. S3) for the data from the amperograms in Fig. 2. The relationship of Q vs. $t^{½}$ was fitted by linear regression, and the parameters of the corresponding linear equations are listed in Table 1. The obtained R^2 values indicate that there is a linear correlation in the plot of Q vs. $t^{½}$ (Table 1). According to the experimental conditions, it was not expected that oxidation of SARS-CoV-2 spike glycoprotein can occur at the potential of +600 mV. However, the interaction of SARS-CoV-2 spike glycoprotein with

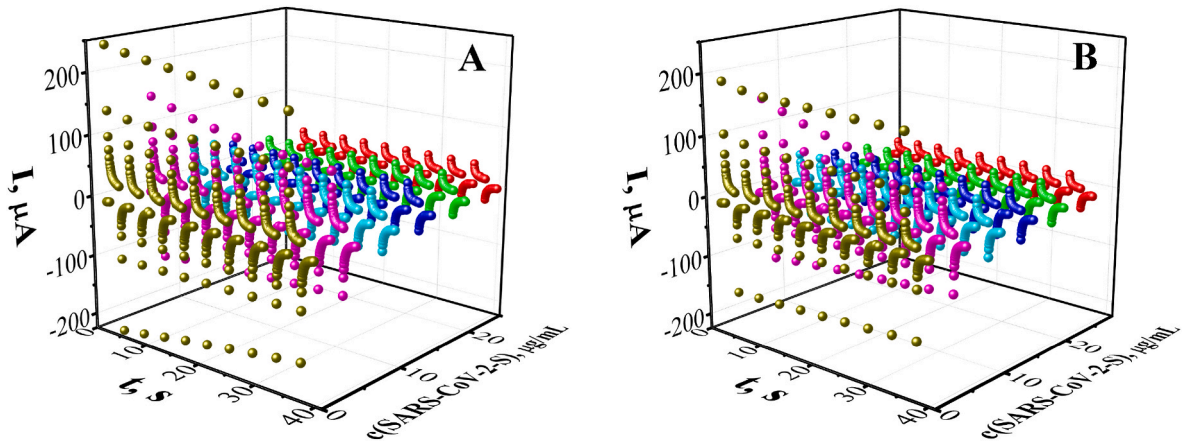

Fig. 1. Pulsed amperometry-based evaluation of MIP-Ppy and NIP-Ppy modified electrodes performed by the potential pulse sequence (+0.6 V and 0 V potentials), representing the incubation process of the SARS-CoV-2 spike glycoprotein. Amperograms were obtained at Pt electrode modified: **A)** with MIP-Ppy modified electrode and **B)** with NIP-Ppy modified electrode in PBS with 0.1 M of KCl, pH 7.4 in the absence of SARS-CoV-2 spike glycoprotein or the presence of SARS-CoV-2 spike glycoprotein concentrations from 5 μg/mL up to 25 μg/mL.

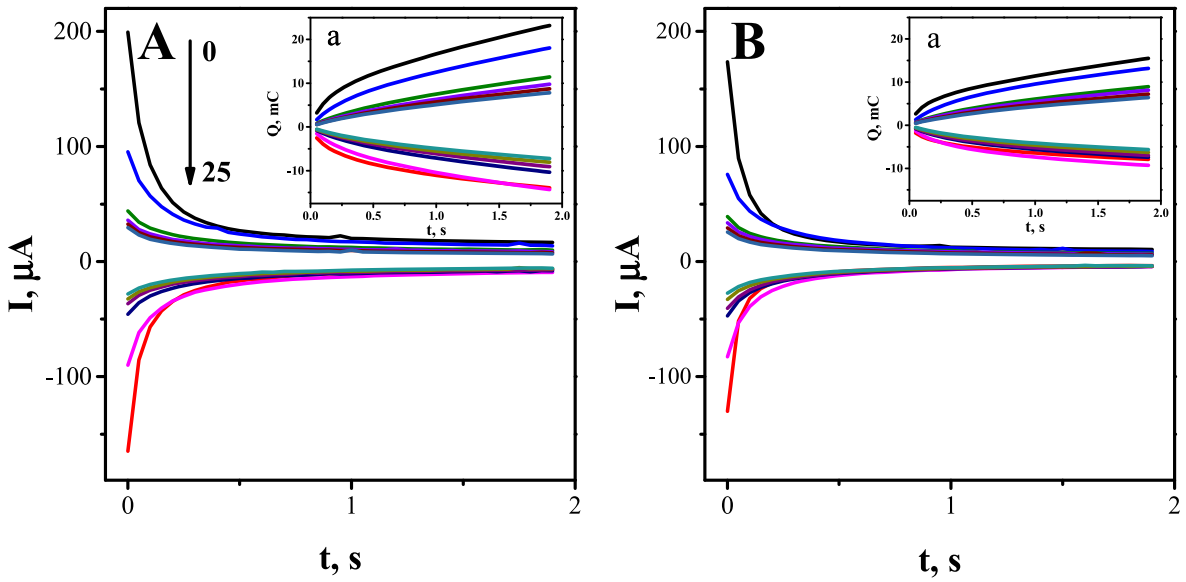

Fig. 2. Amperometric responses were registered during the last (10th) potential pulse of the applied potential pulse sequence (+0.6 V and 0 V potentials), for **A** – MIP-Ppy modified electrode and **B** – NIP-Ppy modified electrode in the absence of SARS-CoV-2 spike glycoprotein and in the presence of SARS-CoV-2 spike glycoprotein from 5 μg/mL up to 25 μg/mL in PBS with 0.1 M of KCl, pH 7.4. The insets (a) represent the change of charge (Q, mC vs. t, s) of the corresponding amperograms.

Table 1
Linear regression parameters of the Anson plot (*Q*, mC vs. $t^{½}$, $s^{½}$) (derived from on the MIP-Ppy and NIP-Ppy modified Pt electrodes for the last (10th) pulse of the potential pulse sequence.

y = ax + b C, μg/mL		MIP-Ppy modified electrode			NIP-Ppy modified electrode		
		a	b	R^2	a	b	R^2
0	+600 mV	16.35	0.46	0.99	10.26	1.22	0.99
	0 V	−8.09	−2.87	0.99	−4.17	−2.22	0.99
5	+600 mV	13.99	−1.39	0.99	9.70	−0.19	0.99
	0 V	−10.48	0.095	0.99	−5.56	−1.74	0.99
10	+600 mV	9.84	−2.27	0.99	7.37	−1.29	0.99
	0 V	−8.39	1.25	0.99	−5.10	−0.46	0.99
15	+600 mV	8.61	−2.22	0.99	6.83	−1.32	0.99
	0 V	−7.57	1.40	0.99	−4.97	−0.20	0.99
20	+600 mV	7.65	−1.91	0.99	6.12	−1.26	0.99
	0 V	−6.68	1.14	0.99	−4.61	0.03	0.99
25	+600 mV	6.85	−1.69	0.99	5.47	−1.13	0.99
	0 V	−5.98	1.05	0.99	−4.22	0.12	0.99

carboxyl, carbonyl, and hydroxyl groups, formed during partial over-oxidation of formed polypyrrole structure and complementary arranged in imprinted cavities was playing an important role in the recognition of SARS-CoV-2 spike glycoprotein and the formation of Ppy/SARS-CoV-2 spike glycoprotein complex, similarly, as it was described for the small molecular weight molecules [68,69]. Due to the replacement of water molecules by SARS-CoV-2 spike glycoprotein, changes in registered current are observed after the incubation of the MIP-Ppy modified electrode in SARS-CoV-2 spike glycoprotein-containing solutions.

Fig. 3A (for MIP-Ppy modified electrode) and Fig. 3D (for NIP-Ppy modified electrode) demonstrate the plots of *Q* vs. $t^{1/2}$ of +600 mV and 0 V pulses. The linear dependence of the slope on the concentration of SARS-CoV-2 spike glycoprotein is represented in Fig. 3B (for MIP-Ppy modified electrode) and Fig. 3E (for NIP-Ppy modified electrode). The plots represented in Fig. 3 illustrate that slope values are very different for MIP-Ppy and NIP-Ppy modified electrodes under the same experimental conditions. The linear dependence of the slope value on the concentration of the analyte for the MIP-Ppy modified electrode (−0.387 for +600 mV pulse and 0.1303 for 0 mV pulse (Fig. 3B)) is steeper than for the NIP-Ppy modified electrode (−0.2015 for +600 mV pulse and 0.0156 for 0 mV pulse (Fig. 3E)). This confirms that the analyte tends to interact stronger with the MIP-Ppy than with the NIP-Ppy. A positive value of the intercept was calculated only in the case where MIP-Ppy and NIP-Ppy modified Pt electrodes were incubated in SARS-CoV-2 spike glycoprotein-free PBS solution (Table 1, Fig. 3C and F). When the concentration of SARS-CoV-2 spike glycoprotein in the solution was increased, all obtained intercept values became negative. A plausible explanation of the observed effect was given by Plausinaitis et al. [63]. The mentioned work describes the quartz crystal microbalance-based evaluation of the electrochemical formation of an aggregated polypyrrole layer. Concerning some other reports [70,71], it was assumed that the pyrrole oxidation process is occurring according to the principles described by heterogeneous kinetics. Here described study is based on the operating principles of the MIP. This means the formation of the complementary cavities in the polymer in the stage of polymerization and the attendance of these cavities in the specific interaction with the analyte during the evaluation step. Thus, molecules adsorbed on the Ppy surface hinder the heterogeneous pyrrole oxidation and reduction reaction.

Data presented in Fig. 3B and E illustrate that the slope *k* of the Anson equation, which was calculated according to equation (1), decreases by increasing the concentration of SARS-CoV-2 spike glycoprotein. At the electrode potential of +600 mV, this effect is much more distinct in comparison to that at 0 mV potential. The slope '*k*', which is indicated by equation (1), is related to (i) the equivalent number of electrons '*n*', which is transferred during the electrochemical reaction; (ii) electrochemically active area '*A* '; concentration of material '*C*' and diffusion coefficient '*D*'. In our case, this dependence of slope '*k*' on the concentration '*C*' of glycoprotein is related to the decrease of electrochemically active area '*A*'. This conclusion is based on the estimation that values of *n* and *D* parameters are constant at all here evaluated concentrations of SARS-CoV-2 spike glycoprotein because the concentration of all other components in the solution and, therefore, physicochemical characteristics (e.g., density and viscosity) are the same. It should be noted that in the case of the MIP-Ppy modified electrode, the dependence of '*k*' on the concentration of SARS-CoV-2 spike glycoprotein is more significantly expressed in comparison to that of the NIP-Ppy modified electrode. At the first glance, taking into account that the dependence of 'k' on the concentration of SARS-CoV-2 spike glycoprotein '*C*' is linear, it was determined that the dependence of '*k*' value on *C* is 1.9 times more

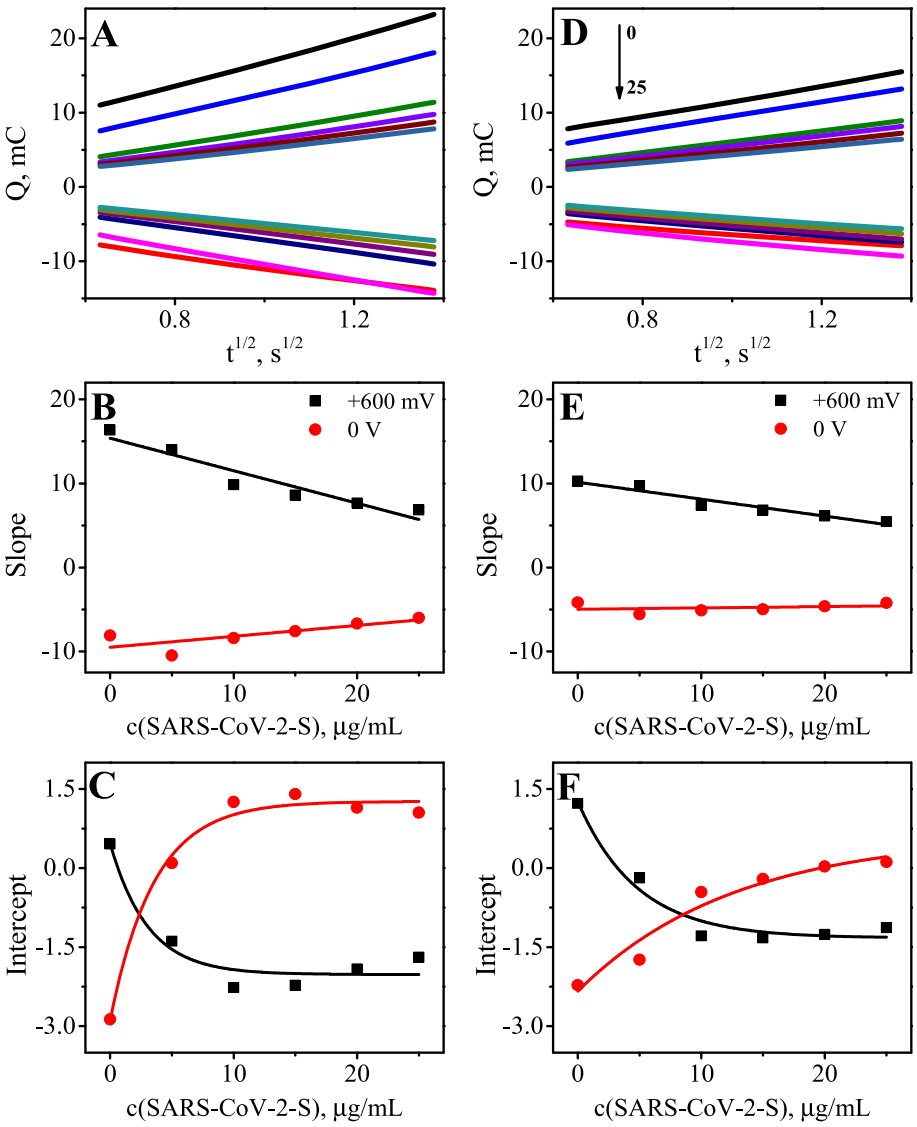

Fig. 3. A and **D** represent the Anson plots (*Q*, mC vs. $t^{½}$, $s^{½}$) derived from the amperometric response registered during the last (10th) potential pulse of the applied potential pulse sequence (+0.6 V and 0 V potentials), presented in Fig. 2 for **A** – MIP-Ppy modified electrode and **D** – NIP-Ppy modified electrode. **B** and **E** represent the slope values of the linear regression equation $y = ax + b$ (from) vs. the concentration of SARS-CoV-2 spike glycoprotein (concentration, μg/mL). **C** and **F** represent the intercept of the same linear regression values (from Table 1) vs. the concentration of SARS-CoV-2 spike glycoprotein (μg/mL).

strongly expressed in the case of MIP-Ppy modified electrode in comparison to that value of NIP-Ppy modified electrode at +600 mV. This fact enables us to conclude that according to the slope, the active area of MIP-Ppy ($A_{MIP\text{-}Ppy}$) is 1.9 times larger in comparison to that area of NIP-Ppy ($A_{NIP\text{-}Ppy}$).

A schematic representation of action, which represent results determined by chronoamperometry, is presented in Fig. 4. As it was discussed above, the decrease of surface charge at higher concentrations of SARS-CoV-2 spike glycoprotein is related to the blocking of MIP-Ppy surface by dielectric material – SARS-CoV-2 spike glycoprotein. All electrical charge passing during this chronoamperometric experiment is determined by adsorption/desorption of ions on MIP-Ppy or NIP-Ppy layers and by doping/dedoping of Ppy-based layers by anions such as PO_4^{3-}, HPO_4^{2-}, $H_2PO_4^-$ and Cl^-. Therefore, SARS-CoV-2 spike glycoprotein adsorbed on the Ppy surface forms a significant barrier for the adsorption/desorption of ions on the MIP-Ppy layer and by doping/dedoping of the MIP-Ppy layer by anions. Fig. 4A and C well represent results that could be determined by experiment when in solution and on the surface of modified electrode SARS-CoV-2 spike glycoprotein concentration is equal to 0 μg/mL. Therefore, in this case, the adsorption/desorption of ions on MIP-Ppy or NIP-Ppy layers and doping/dedoping of Ppy-based layers is more intensive in comparison to the MIP-Ppy layer. On the contrary, schematics represented in Fig. 4B and D illustrate the interaction of Ppy-based layers with SARS-CoV-2 spike glycoprotein and, respectively, partial blocking of the Ppy surface.

In this context, according to the Anson plot-based evaluation, a SARS-CoV-2 spike glycoprotein molecule is an analyte that is interacting with MIP-Ppy and nonspecifically adsorbing on NIP-Ppy layers.

Fig. 5 represents the calibration plot based on ΔQ values vs. logarithm of the concentration of SARS-CoV-2 spike glycoprotein in PBS solution, pH 7.4. The calibration plot (Fig. 5) of the described system has a linear relationship.

$$y = Ax + B$$

The obtained functions of the linear relationships were as follows: y = 24.3599x-11.0234, with R^2 = 09497 (for MIP-Ppy modified electrode) and y = 14.3361x-8.4771 with R^2 = 0.9591 (for NIP-Ppy modified electrode). The linear relationship, in the PBS in absence of SARS-CoV-2 spike glycoprotein (c(SARS-CoV-2-S) = x = 0 μg/mL), represents the lowest change of charge (mC). The charge passed through MIP-Ppy at the initial point was higher than that through NIP-Ppy. This effect is explained by the complementary cavities in the polymer. The presence of the complementary cavities enables the faster charge transfer after extraction of the SARS-CoV-2 spike glycoprotein from the MIP-Ppy layer. After the MIP-Ppy and NIP-Ppy modified electrodes were re-incubated in the SARS-CoV-2 spike glycoprotein containing PBS, a

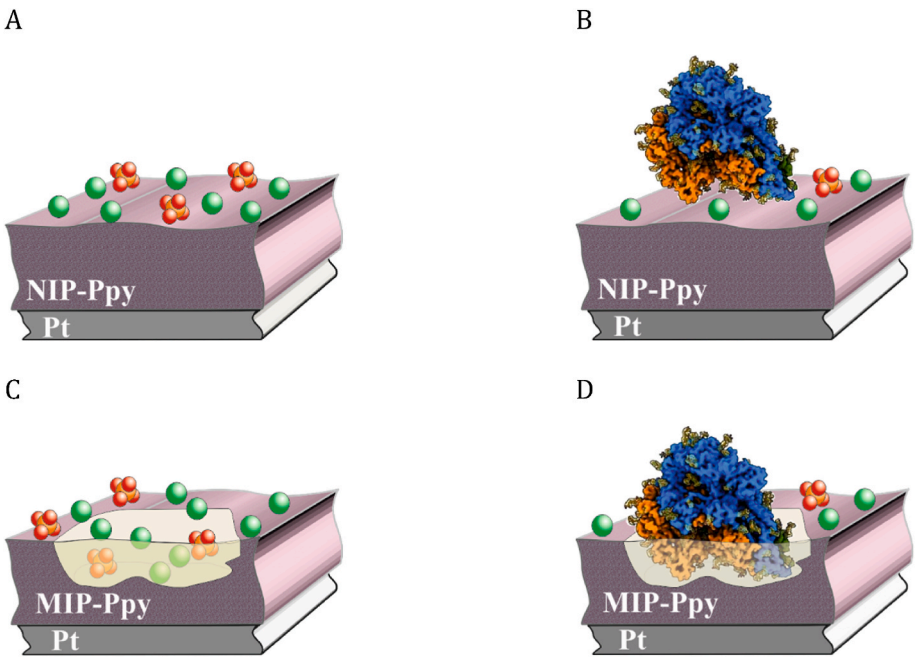

Fig. 4. Interaction of NIP-Ppy and MIP-Ppy with SARS-CoV-2 spike glycoprotein and anions (PO_4^{3-}, HPO_4^{2-}, or $H_2PO_4^-$ and Cl^-). **A** – NIP-Ppy in a solution containing 0 μg/mL of SARS-CoV-2 spike glycoprotein; **B** – NIP-Ppy in a solution containing >0 μg/mL of SARS-CoV-2 spike glycoprotein; **C** – MIP-Ppy in a solution containing 0 μg/mL of SARS-CoV-2 spike glycoprotein; **D** – MIP-Ppy in a solution containing >0 μg/mL of SARS-CoV-2 spike glycoprotein.

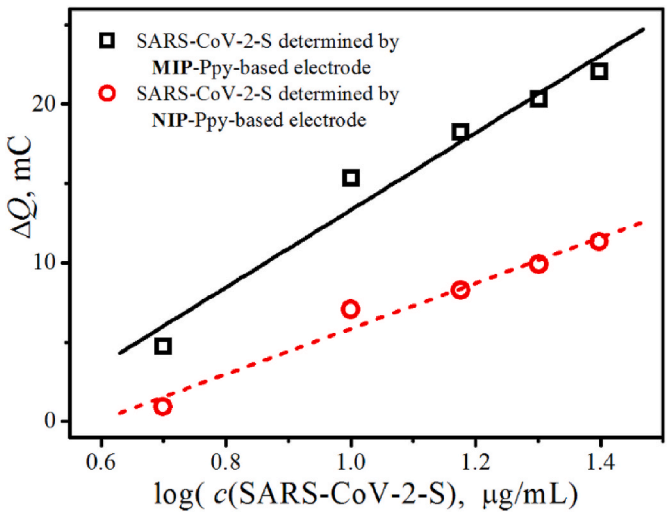

Fig. 5. Calibration curves of MIP-Ppy and NIP-Ppy modified electrodes presented as Δ*Q* vs. logarithm of the concentration of SARS-CoV-2 spike glycoprotein.

significant current drop was observed. The change of charge within the MIP-Ppy layer was observed higher than on the NIP-Ppy layer. This means that the MIP-Ppy modified electrode was more sensitive towards SARS-CoV-2 than the NIP-Ppy modified electrode. The registered charge variations of MIP-Ppy and NIP-Ppy modified electrodes at the highest concentrations of SARS-CoV-2 spike glycoprotein (c(SARS-CoV-2-S) = 25 μg/mL) were very similar. This should indicate that the protein covers the surface of both MIP-Ppy and NIP-Ppy layers, although differences between MIP-Ppy and NIP-Ppy layers were observed.

A comparison of some studies that were assessing the applicability of MIP-based sensors for the detection of SARS-CoV-2 proteins is demonstrated in Table 2.

The described method applied for the evaluation of the interaction between SARS-CoV-2 spike glycoproteins and the MIP-Ppy modified electrode has significant advantages and the most important is that those insights about the interaction are concluded by the evaluation of PAD results. This means that the detection of SARS-CoV-2 spike glycoproteins can be performed by the assessment of Anson plot. Therefore, we believe, that the Anson plot is a simple and handy method for quick assessment the adsorption process on the electrode MIP-modified electrode.

4. Conclusions

After the MIP-Ppy and NIP-Ppy modified electrodes were incubated for the first time in the SARS-CoV-2 spike glycoprotein containing PBS, a significant current drop was observed. Based on the total charge vs. square of time plots (the Anson plots), the interaction between SARS-CoV-2 spike glycoproteins and the molecularly imprinted polypyrrole was assessed. Based on the dependence of the Anson plot's slope values on the concentration of the glycoproteins, we declare that glycoproteins adsorb more strongly on MIP-Ppy than on NIP-Ppy. Moreover, taking into the account the Anson plot-based evaluation it was concluded that, the SARS-CoV-2 spike glycoprotein molecule is an analyte, which is interacting with MIP-Ppy and at some extent non-specifically adsorbing on NIP-Ppy. Therefore, Anson plot-based calculations are valuable for determining the interaction between SARS-CoV-2 spike glycoproteins and molecularly imprinted polypyrrole (MIP-Ppy). Further, the calibration curve of current values was depicted for glycoprotein concentrations in the range from 0 μg/mL to 25 μg/mL. The calibration plot of the described system has a form of exponential decay. The current drop registered by the MIP-Ppy modified electrode was significantly higher than that determined by the NIP-Ppy modified electrode. This means that the MIP-Ppy modified electrode was more sensitive towards SARS-CoV-2 spike glycoprotein than the NIP-Ppy modified electrode. The current value observed in the calibration curve for the MIP-Ppy modified electrode at the initial point (glycoprotein concentration was 0 μg/mL) was 1.36 times higher in comparison with that of the NIP-Ppy modified electrode. This phenomenon occurred due to the presence of the complementary cavities in Ppy that were formed after the extraction of SARS-CoV-2 spike glycoprotein from MIP-Ppy. This observation can also

Table 2
MIP-based sensors used for the detection of SARS-CoV-2 proteins.

Electrode	Polymer	Analyte	Method of analysis	Comments	Ref.
Gold-based thin-film electrode	Poly(*m*-phenylenediamine)	SARS-CoV-2 nucleoprotein	DPV	Analyzed by using a redox probe; LOD 15 fM	[52]
macroporous gold screen-printed electrode	Poly(*o*-phenylenediamine)	SARS-CoV-2 receptor-binding domain	EIS	Analyzed by using a redox probe; LOD 0.7 pg mL^{-1}	[53]
Disposable thin-film metal electrode	Poly(3-aminophenylboronic acid)	SARS-CoV-2 spike protein subunit S1	SWV[a]	Analyzed by using a redox probe; LOD 15 fM	[54]
Gold SPRi chip	Poly(scopoletin)	SARS-CoV-2 receptor binding domain	SPRi[b]	Peptide epitope-imprinted polymer microarrays	[55]
Glassy carbon electrode	Polypyrrole-poly(3-aminophenyl boronic acid)	SARS-CoV-2 antigen	DPV, CA[c]	Graphene was added to the polymer composition; Analyzed by using a redox probe; LOD 0.326 fg mL^{-1}	[56]
Platinum electrode	Polypyrrole	SARS-CoV-2 Spike Glycoprotein	CA	No redox probe was used during CA.	[45]

[a] – square wave voltammetry.
[b] – surface plasmon resonance imaging.
[c] – chronoamperometry.

serve as the validation for the formation of MIP-Ppy. This technique can be applied to the development of a sensor for the diagnosis of a SARS-CoV-2 infection.

Credit author statement

Vilma Ratautaite – Methodology, investigation, data analysis, writing – original draft, writing – review & editing, interpretation of data; Raimonda Boguzaite – Methodology, investigation, data analysis, writing – original draft, interpretation of data, data analysis; E**rnestas Brazys** – Methodology, investigation, data analysis, writing – original draft, interpretation of data, data analysis; D**eivis Plausinaitis** – data analysis, interpretation of data, writing – review & editing; S**imonas Ramanavicius** – Writing – review & editing, data analysis, interpretation of data; U**rte Samukaite-Bubniene** – Writing – review & editing; data analysis, interpretation of data; **Mikhael Bechelany** – Writing - review & editing; **Arunas Ramanavicius** – Interpretation of data, data analysis, supervision, conceptualization, writing – review & editing, funding acquisition.

Declaration of competing interest

The authors declare that they have no known competing financial interests or personal relationships that could have appeared to influence the work reported in this paper.

Data availability

Data will be made available on request.

Acknowledgments

This project has received funding from the Research Council of Lithuania (LMTLT), GILIBERT 2021 program agreement No S-LZ-21-4 and was co-founded by Campus France grant No. 46593RA (PHC GILIBERT 2021).

Appendix A. Supplementary data

Supplementary data to this article can be found online at https://doi.org/10.1016/j.talanta.2022.123981.

References

[1] V. Ratautaite, U. Samukaite-Bubniene, D. Plausinaitis, R. Boguzaite, D. Balciunas, A. Ramanaviciene, G. Neunert, A. Ramanavicius, Molecular imprinting technology for determination of uric acid, Int. J. Mol. Sci. 22 (2021) 5032, https://doi.org/10.3390/ijms22095032.
[2] S. Ramanavicius, A. Jagminas, A. Ramanavicius, Advances in molecularly imprinted polymers based affinity sensors (review), Polymers (Basel) 13 (2021) 974, https://doi.org/10.3390/polym13060974.
[3] S. Ramanavicius, A. Ramanavicius, Conducting polymers in the design of biosensors and biofuel cells, Polymers 13 (2021) 49, https://doi.org/10.3390/polym13010049.
[4] V. Ratautaite, S.D. Janssens, K. Haenen, M. Nesládek, A. Ramanaviciene, I. Baleviciute, A. Ramanavicius, Molecularly imprinted polypyrrole based impedimentric sensor for theophylline determination, Electrochim. Acta 130 (2014) 361–367, https://doi.org/10.1016/j.electacta.2014.03.035.
[5] V. Ratautaite, M. Nesladek, A. Ramanaviciene, I. Baleviciute, A. Ramanavicius, Evaluation of histamine imprinted polypyrrole deposited on boron doped nanocrystalline diamond, Electroanalysis 26 (2014) 2458–2464, https://doi.org/10.1002/elan.201400294.
[6] V. Ratautaite, D. Plausinaitis, I. Baleviciute, L. Mikoliunaite, A. Ramanaviciene, A. Ramanavicius, Characterization of caffeine-imprinted polypyrrole by a quartz crystal microbalance and electrochemical impedance spectroscopy, Sens. Actuat. B-Chem. 212 (2015) 63–71, https://doi.org/10.1016/j.snb.2015.01.109.
[7] M. Peeters, F.J. Troost, B. van Grinsven, F. Horemans, J. Alenus, M.S. Murib, D. Keszthelyi, A. Ethirajan, R. Thoelen, T.J. Cleij, P. Wagner, MIP-based biomimetic sensor for the electronic detection of serotonin in human blood plasma, Sens. Actuat. B-Chem. 171–172 (2012) 602–610, https://doi.org/10.1016/j.snb.2012.05.040.
[8] G. Bagdžiūnas, Theoretical design of molecularly imprinted polymers based on polyaniline and polypyrrole for detection of tryptophan, Mol. Syst. Des. Eng. 5 (2020) 1504–1512, https://doi.org/10.1039/D0ME00089B.
[9] A.K. Roy, N.V. S, C. Dhand, B.D. Malhotra, Molecularly imprinted polyaniline film for ascorbic acid detection, J. Mol. Recogn. 24 (2011) 700–706, https://doi.org/10.1002/jmr.1104.
[10] Y. Kong, J.H. Ni, W.C. Wang, Z.D. Chen, Enantioselective recognition of amino acids based on molecularly imprinted polyaniline electrode column, Electrochim. Acta 56 (2011) 4070–4074, https://doi.org/10.1016/j.electacta.2011.01.120.
[11] Z. Mazouz, S. Rahali, N. Fourati, C. Zerrouki, N. Aloui, M. Seydou, N. Yaakoubi, M. M. Chehimi, A. Othmane, R. Kalfat, Highly selective polypyrrole MIP-based gravimetric and electrochemical sensors for picomolar detection of glyphosate, Sensors (Basel) 17 (2017) 2586, https://doi.org/10.3390/s17112586.
[12] J.M. Kim, J.C. Yang, J.Y. Park, Quartz crystal microbalance (QCM) gravimetric sensing of theophylline via molecularly imprinted microporous polypyrrole copolymers, Sens. Actuat. B-Chem. 206 (2015) 50–55, https://doi.org/10.1016/j.snb.2014.09.047.
[13] D. Plausinaitis, L. Sinkevicius, U. Samukaite-Bubniene, V. Ratautaite, A. Ramanavicius, Evaluation of electrochemical quartz crystal microbalance based sensor modified by uric acid-imprinted polypyrrole, Talanta 220 (2020), 121414, https://doi.org/10.1016/j.talanta.2020.121414.
[14] R.D. Crapnell, N.C. Dempsey-Hibbert, M. Peeters, A. Tridente, C.E. Banks, Molecularly imprinted polymer based electrochemical biosensors: overcoming the challenges of detecting vital biomarkers and speeding up diagnosis, Talanta Open 2 (2020), 100018, https://doi.org/10.1016/j.talo.2020.100018.
[15] J.W. Lowdon, H. Diliën, P. Singla, M. Peeters, T.J. Cleij, B. van Grinsven, K. Eersels, MIPs for commercial application in low-cost sensors and assays – an overview of the current status quo, Sens. Actuat. B-Chem. 325 (2020), 128973, https://doi.org/10.1016/j.snb.2020.128973.
[16] A. Yarman, F.W. Scheller, How reliable is the electrochemical readout of MIP sensors? Sensors (Basel) 20 (2020) 2677, https://doi.org/10.3390/s20092677.
[17] E.N. Ndunda, Molecularly imprinted polymers—a closer look at the control polymer used in determining the imprinting effect: a mini review, J. Mol. Recogn. 33 (2020), e2855, https://doi.org/10.1002/jmr.2855.

[18] P.S. Sharma, A. Garcia-Cruz, M. Cieplak, K.R. Noworyta, W. Kutner, 'Gate effect' in molecularly imprinted polymers: the current state of understanding, Curr. Opin. Electrochem. 16 (2019) 50–56, https://doi.org/10.1016/j.coelec.2019.04.020.

[19] J. Erdőssy, V. Horváth, A. Yarman, F.W. Scheller, R.E. Gyurcsányi, Electrosynthesized molecularly imprinted polymers for protein recognition, TRAC-Trends Anal. Chem. 79 (2016) 179–190, https://doi.org/10.1016/j.trac.2015.12.018.

[20] X. Kan, Z. Xing, A. Zhu, Z. Zhao, G. Xu, C. Li, H. Zhou, Molecularly imprinted polymers based electrochemical sensor for bovine hemoglobin recognition, Sens. Actuat. B-Chem. 168 (2012) 395–401, https://doi.org/10.1016/j.snb.2012.04.043.

[21] R. Viveiros, S. Rebocho, T. Casimiro, Green strategies for molecularly imprinted polymer development, Polymers (Basel) 10 (2018) 306, https://doi.org/10.3390/polym10030306.

[22] Q. Zeng, X. Huang, M. Ma, A molecularly imprinted electrochemical sensor based on polypyrrole/carbon nanotubes composite for the detection of S-ovalbumin in egg white, Int. J. Electrochem. Sci. 12 (2017) 3965–3981, https://doi.org/10.20964/2017.05.61.

[23] Z. Stojanovic, J. Erdőssy, K. Keltai, F.W. Scheller, R.E. Gyurcsányi, Electrosynthesized molecularly imprinted polyscopoletin nanofilms for human serum albumin detection, Anal. Chim. Acta 977 (2017) 1–9, https://doi.org/10.1016/j.aca.2017.04.043.

[24] Y. Lai, C. Zhang, Y. Deng, G. Yang, S. Li, C. Tang, N. He, A novel α-fetoprotein-MIP immunosensor based on AuNPs/PTh modified glass carbon electrode, Chin. Chem. Lett. 30 (2019) 160–162, https://doi.org/10.1016/j.cclet.2018.07.011.

[25] A. Yarman, D. Dechtrirat, M. Bosserdt, K.J. Jetzschmann, N. Gajovic-Eichelmann, F.W. Scheller, Cytochrome c-derived hybrid systems based on moleculary imprinted polymers, Electroanalysis 27 (2015) 573–586, https://doi.org/10.1002/elan.201400592.

[26] L.-W. Qian, X.-L. Hu, P. Guan, B. Gao, D. Wang, C.-L. Wang, J. Li, C.-B. Du, W.-Q. Song, Thermal preparation of lysozyme-imprinted microspheres by using ionic liquid as a stabilizer, Anal. Bioanal. Chem. 406 (2014) 7221–7231, https://doi.org/10.1007/s00216-014-8133-9.

[27] S. Wu, W. Tan, H. Xu, Protein molecularly imprinted polyacrylamide membrane: for hemoglobin sensing, Analyst 135 (2010) 2523–2527, https://doi.org/10.1039/C0AN00191K.

[28] V.K. Tamboli, N. Bhalla, P. Jolly, C.R. Bowen, J.T. Taylor, J.L. Bowen, C. J. Allender, P. Estrela, Hybrid synthetic receptors on MOSFET devices for detection of prostate specific antigen in human plasma, Anal. Chem. 88 (2016) 11486–11490, https://doi.org/10.1021/acs.analchem.6b02619.

[29] P. Karami, H. Bagheri, M. Johari-Ahar, H. Khoshsafar, F. Arduini, A. Afkhami, Dual-modality impedimetric immunosensor for early detection of prostate-specific antigen and myoglobin markers based on antibody-molecularly imprinted polymer, Talanta 202 (2019) 111–122, https://doi.org/10.1016/j.talanta.2019.04.061.

[30] V.V. Shumyantseva, T.V. Bulko, L.V. Sigolaeva, A.V. Kuzikov, A.I. Archakov, Electrosynthesis and binding properties of molecularly imprinted poly-o-phenylenediamine for selective recognition and direct electrochemical detection of myoglobin, Biosens. Bioelectron. 86 (2016) 330–336, https://doi.org/10.1016/j.bios.2016.05.101.

[31] F.T.C. Moreira, S. Sharma, R.A.F. Dutra, J.P.C. Noronha, A.E.G. Cass, M.G.F. Sales, Protein-responsive polymers for point-of-care detection of cardiac biomarker, Sens. Actuat. B-Chem. 196 (2014) 123–132, https://doi.org/10.1016/j.snb.2014.01.038.

[32] F.T.C. Moreira, R.A.F. Dutra, J.P.C. Noronha, M.G.F. Sales, Electrochemical biosensor based on biomimetic material for myoglobin detection, Electrochim. Acta 107 (2013) 481–487, https://doi.org/10.1016/j.electacta.2013.06.061.

[33] A. Ramanaviciene, A. Ramanavicius, Molecularly imprinted polypyrrole-based synthetic receptor for direct detection of bovine leukemia virus glycoproteins, Biosens. Bioelectron. 20 (2004) 1076–1082, https://doi.org/10.1016/j.bios.2004.05.014.

[34] B. Babamiri, A. Salimi, R. Hallaj, A molecularly imprinted electrochemiluminescence sensor for ultrasensitive HIV-1 gene detection using EuS nanocrystals as luminophore, Biosens. Bioelectron. 117 (2018) 332–339, https://doi.org/10.1016/j.bios.2018.06.003.

[35] V. Ratautaite, S.N. Topkaya, L. Mikoliunaite, M. Ozsoz, Y. Oztekin, A. Ramanaviciene, A. Ramanavicius, Molecularly imprinted polypyrrole for DNA determination, Electroanalysis 25 (2013) 1169–1177, https://doi.org/10.1002/elan.201300063.

[36] A.A. Lahcen, F. Arduini, F. Lista, A. Amine, Label-free electrochemical sensor based on spore-imprinted polymer for Bacillus cereus spore detection, Sens. Actuat. B-Chem. 276 (2018) 114–120, https://doi.org/10.1016/j.snb.2018.08.031.

[37] S. Chen, X. Chen, L. Zhang, J. Gao, Q. Ma, Electrochemiluminescence detection of Escherichia coli O157:H7 based on a novel polydopamine surface imprinted polymer biosensor, ACS Appl. Mater. Interfaces 9 (2017) 5430–5436, https://doi.org/10.1021/acsami.6b12455.

[38] Z. Iskierko, P.S. Sharma, K. Bartold, A. Pietrzyk-Le, K. Noworyta, W. Kutner, Molecularly imprinted polymers for separating and sensing of macromolecular compounds and microorganisms, Biotechnol. Adv. 34 (2016) 30–46, https://doi.org/10.1016/j.biotechadv.2015.12.002.

[39] Z. Wang, F. Li, J. Xia, L. Xia, F. Zhang, S. Bi, G. Shi, Y. Xia, J. Liu, Y. Li, L. Xia, An ionic liquid-modified graphene based molecular imprinting electrochemical sensor for sensitive detection of bovine hemoglobin, Biosens. Bioelectron. 61 (2014) 391–396, https://doi.org/10.1016/j.bios.2014.05.043.

[40] L. Li, L. Yang, Z. Xing, X. Lu, X. Kan, Surface molecularly imprinted polymers-based electrochemical sensor for bovine hemoglobin recognition, Analyst 138 (2013) 6962–6968, https://doi.org/10.1039/C3AN01435E.

[41] H.-J. Chen, Z.-H. Zhang, L.-J. Luo, S.-Z. Yao, Surface-imprinted chitosan-coated magnetic nanoparticles modified multi-walled carbon nanotubes biosensor for detection of bovine serum albumin, Sens. Actuat. B-Chem. 163 (2012) 76–83, https://doi.org/10.1016/j.snb.2012.01.010.

[42] Z. Mazouz, M. Mokni, N. Fourati, C. Zerrouki, F. Barbault, M. Seydou, R. Kalfat, N. Yaakoubi, A. Omezzine, A. Bouslema, A. Othmane, Computational approach and electrochemical measurements for protein detection with MIP-based sensor, Biosens. Bioelectron. 151 (2020), 111978, https://doi.org/10.1016/j.bios.2019.111978.

[43] M.L. Yola, N. Atar, Development of cardiac troponin-I biosensor based on boron nitride quantum dots including molecularly imprinted polymer, Biosens. Bioelectron. 126 (2019) 418–424, https://doi.org/10.1016/j.bios.2018.11.016.

[44] B.V.M. Silva, B.A.G. Rodríguez, G.F. Sales, M.D.P.T. Sotomayor, R.F. Dutra, An ultrasensitive human cardiac troponin T graphene screen-printed electrode based on electropolymerized-molecularly imprinted conducting polymer, Biosens. Bioelectron. 77 (2016) 978–985, https://doi.org/10.1016/j.bios.2015.10.068.

[45] V. Ratautaite, R. Boguzaite, E. Brazys, A. Ramanaviciene, E. Ciplys, M. Juozapaitis, R. Slibinskas, M. Bechelany, A. Ramanavicius, Molecularly imprinted polypyrrole based sensor for the detection of SARS-CoV-2 spike glycoprotein, Electrochim. Acta 403 (2022) 139–581, https://doi.org/10.1016/j.electacta.2021.139581.

[46] R.A. Dorledo de Faria, L.G. Dias Heneine, T. Matencio, Y. Messaddeq, Faradaic and non-faradaic electrochemical impedance spectroscopy as transduction techniques for sensing applications, Int. J. Bios. Bioelectron 5 (2019) 29–31, https://doi.org/10.15406/ijbsbe.2019.05.00148.

[47] J. Heinze, B.A. Frontana-Uribe, S. Ludwigs, Electrochemistry of conducting polymers—persistent models and new concepts, Chem. Rev. 110 (2010) 4724–4771, https://doi.org/10.1021/cr900226k.

[48] M.F. Suárez, R.G. Compton, In situ atomic force microscopy study of polypyrrole synthesis and the volume changes induced by oxidation and reduction of the polymer, J. Electroanal. Chem. 462 (1999) 211–221, https://doi.org/10.1016/S0022-0728(98)00414-8.

[49] M.R. Gandhi, P. Murray, G.M. Spinks, G.G. Wallace, Mechanism of electromechanical actuation in polypyrrole, Synth. Met. 73 (1995) 247–256, https://doi.org/10.1016/0379-6779(95)80022-0.

[50] T.F. Otero, E. Angulo, Oxidation-reduction of polypyrrole films. Kinetics, structural model and applications, Solid State Ion 63–65 (1993) 803–809, https://doi.org/10.1016/0167-2738(93)90200-M.

[51] O.I. Parisi, M. Dattilo, F. Patitucci, R. Malivindi, V. Pezzi, I. Perrotta, M. Ruffo, F. Amone, F. Puoci, "Monoclonal-type" plastic antibodies for SARS-CoV-2 based on molecularly imprinted polymers, bioRxiv (2020), https://doi.org/10.1101/2020.05.28.120709, 2020.2005.2028.120709.

[52] A. Raziq, A. Kidakova, R. Boroznjak, J. Reut, A. Öpik, V. Syritski, Development of a portable MIP-based electrochemical sensor for detection of SARS-CoV-2 antigen, Biosens. Bioelectron. 178 (2021), 113029, https://doi.org/10.1016/j.bios.2021.113029.

[53] M.A. Tabrizi, J.P. Fernández-Blázquez, D.M. Medina, P. Acedo, An ultrasensitive molecularly imprinted polymer-based electrochemical sensor for the determination of SARS-CoV-2-RBD by using macroporous gold screen-printed electrode, Biosens. Bioelectron. 196 (2021), 113729, https://doi.org/10.1016/j.bios.2021.113729.

[54] A.G. Ayankojo, R. Boroznjak, J. Reut, A. Öpik, V. Syritski, Molecularly imprinted polymer based electrochemical sensor for quantitative detection of SARS-CoV-2 spike protein, Sens. Actuat. B-Chem. 353 (2022), 131160, https://doi.org/10.1016/j.snb.2021.131160.

[55] Z. Bognár, E. Supala, A. Yarman, X. Zhang, F.F. Bier, F. Scheller, R.E. Gyurcsányi, Peptide epitope-imprinted polymer microarrays for selective protein recognition. Application for SARS-CoV-2 RBD protein, Chem. Sci. 13 (2022) 1263–1269, https://doi.org/10.1039/D1SC04502D.

[56] S.A. Hashemi, S. Bahrani, S.M. Mousavi, N. Omidifar, N.G.G. Behbahan, M. Arjmand, S. Ramakrishna, K.B. Lankarani, M. Moghadami, M. Firoozsani, Graphene-based femtogram-level sensitive molecularly imprinted polymer of SARS-CoV-2, Adv. Mater. Interfaces 8 (2021), 2101466, https://doi.org/10.1002/admi.202101466.

[57] N. Cennamo, G. D'Agostino, C. Perri, F. Arcadio, G. Chiaretti, E.M. Parisio, G. Camarlinghi, C. Vettori, F. Di Marzo, R. Cennamo, G. Porto, L. Zeni, Proof of concept for a quick and highly sensitive on-site detection of SARS-CoV-2 by plasmonic optical fibers and molecularly imprinted polymers, Sensors 21 (2021) 1681, https://doi.org/10.3390/s21051681.

[58] G. Jamalipour Soufi, S. Iravani, R.S. Varma, Molecularly imprinted polymers for the detection of viruses: challenges and opportunities, Analyst 146 (2021) 3087–3100, https://doi.org/10.1039/D1AN00149C.

[59] F.C. Anson, Innovations in the study of adsorbed reactants by chronocoulometry, Anal. Chem. 38 (1966) 54–57, https://doi.org/10.1021/ac60233a014.

[60] F.C. Anson, R.A. Osteryoung, Chronocoulometry: a convenient, rapid and reliable technique for detection and determination of adsorbed reactants, J. Chem. Educ. 60 (1983) 293, https://doi.org/10.1021/ed060p293.

[61] F.C. Anson, J.H. Christie, R.A. Osteryoung, A study of the adsorption of cadmium (II) on mercury from thiocyanate solutions by double potential-step chronocoulometry, J. Electroanal. Chem. Interf. Electrochem. 13 (1967) 343–353, https://doi.org/10.1016/0022-0728(67)80037-8.

[62] A. Ramanavicius, Y. Oztekin, A. Ramanaviciene, Electrochemical formation of polypyrrole-based layer for immunosensor design, Sens. Actuat. B-Chem. 197 (2014) 237–243, https://doi.org/10.1016/j.snb.2014.02.072.

[63] D. Plausinaitis, V. Ratautaite, L. Mikoliunaite, L. Sinkevicius, A. Ramanaviciene, A. Ramanavicius, Quartz crystal microbalance-based evaluation of the electrochemical formation of an aggregated polypyrrole particle-based layer, Langmuir 31 (2015) 3186–3193, https://doi.org/10.1021/la504340u.
[64] K. Zhou, H. Wang, Y. Zhang, J. Liu, H. Yan, An advanced technique to evaluate the electrochromic performances of NiO films by multi-cycle double-step potential chronocoulometry, J. Electrochem. Soc. 163 (2016) H1033–H1040, https://doi.org/10.1149/2.1011610jes.
[65] A. García-Miranda Ferrari, C.W. Foster, P.J. Kelly, D.A.C. Brownson, C.E. Banks, Determination of the electrochemical area of screen-printed electrochemical sensing platforms, Biosensors (Basel) 8 (2018) 53, https://doi.org/10.3390/bios8020053.
[66] J. Puy, M. Pla, F. Mas, F. Sanz, Adsorption in double potential step chronocoulometry, J. Electroanal. Chem. Interf. Electrochem. 241 (1988) 89–104, https://doi.org/10.1016/0022-0728(88)85118-0.
[67] G. Bagdžiūnas, A. Ramanavicius, Towards direct enzyme wiring: a theoretical investigation of charge carrier transfer mechanisms between glucose oxidase and organic semiconductors, Phys. Chem. Chem. Phys. 21 (2019) 2968–2976, https://doi.org/10.1039/C8CP07233G.
[68] V. Syritski, J. Reut, A. Menaker, R.E. Gyurcsányi, A. Öpik, Electrosynthesized molecularly imprinted polypyrrole films for enantioselective recognition of l-aspartic acid, Electrochim. Acta 53 (2008) 2729–2736, https://doi.org/10.1016/j.electacta.2007.10.032.
[69] T.C. Tsai, H.Z. Han, C.C. Cheng, L.C. Chen, H.C. Chang, J.J.J. Chen, Modification of platinum microelectrode with molecularly imprinted over-oxidized polypyrrole for dopamine measurement in rat striatum, Sens. Actuat. B-Chem. 171–172 (2012) 93–101, https://doi.org/10.1016/j.snb.2011.07.052.
[70] J.H. Christie, G. Laurer, R.A. Osteryoung, Measurement of charge passed following application of a potential step-application to the study of electrode reactions and adsorption, J. Electroanal. Chem. 7 (1964) 60–72, https://doi.org/10.1016/0022-0728(64)80005-X.
[71] J.H. Christie, G. Lauer, R.A. Osteryoung, F.C. Anson, Determination of charge passed following application of potential step in study of electrode processes, Anal. Chem. 35 (1963), https://doi.org/10.1021/ac60205a003, 1979-1979.